

Performance Characterization for a Small-Aperture Radio-Frequency Pulsar Experiment

Ryan McKnight, Zachary Arnett, Brian C. Peters, Sabrina Ugazio *Ohio University*

BIOGRAPHY

Ryan McKnight is pursuing his Ph.D. in Electrical Engineering and Computer Science at Ohio University as part of the Avionics Engineering Center. His research interests include GNSS inter-constellation time offset determination and radio-frequency pulsar navigation and timing. He was previously involved with development and operations of the Bobcat-1 CubeSat. He received his B.S. in Electrical Engineering from Ohio University in 2019.

Zachary Arnett is pursuing his Ph.D. in Electrical Engineering and Computer Science at Ohio University as part of the Avionics Engineering Center. His research interests include GNSS inter-constellation time offset determination and radio-frequency pulsar navigation and timing. He received his B.S. in Electrical Engineering from Ohio University in 2019.

Brian C. Peters is pursuing his Ph.D. in Electrical Engineering and Computer Science at Ohio University as part of the Avionics Engineering Center. He completed his M.S. in Electrical Engineering at Ohio University in 2021 where he was involved in the development and operation of the Bobcat-1 CubeSat and conducted research on estimation of GNSS inter-constellation time offsets. He was also involved in the development of the Cislunar Autonomous Positioning System demonstration for NASA's CAPSTONE mission.

Sabrina Ugazio is an Assistant Professor in Electrical Engineering and Computer Science at Ohio University. She received her Ph.D. in Electronics and Telecommunications Engineering from Politecnico di Torino in 2013. Her research interests include various aspects of GNSS, such as timing, signal monitoring and remote sensing.

ABSTRACT

While recent studies have suggested the feasibility of radio-frequency (RF) pulsar navigation using reasonably small antenna apertures, as of yet there is no general consensus as to the level of performance that could be achieved by such a system under real-world conditions. Theoretical performance calculations depend on a large number of variables including receiver-specific parameters such as effective antenna aperture, observation time, observation frequency, receiver bandwidth, and noise sources, along with various parameters specific to the pulsar under observation, such as flux density, pulse period, and pulse width. The achievable performance is additionally subject to such real-world constraints as the local radio-frequency interference (RFI) environment, receiver hardware specifications, and available computational power. An experimental approach is therefore necessary to determine a set of reasonable parameters for a practical system, measure the performance that can be achieved using these parameters, and demonstrate the validity of theoretical models.

A previous study described the motivations and preliminary design for such an experiment. This paper serves as a follow-up, providing additional detail about the experiment design. It includes details about site surveys, hardware selection, software algorithms, and error sources that must be accounted for during the data collection, as well as a performance characterization for the experiment. A full consideration of these details is an important step towards using the experiment to validate theoretical performance models.

I. INTRODUCTION

Pulsars are highly magnetized rotating neutron stars that emit high-energy beams of electromagnetic radiation, observed at a distance as a series of pulses (Condon & Ransom, 2016). The pulsed signals emitted by pulsars are highly regular and stable over long periods of time, with certain pulsars even known to rival the stability of atomic clocks (Rawley et al., 1986). This property has led to the use or proposed use of these signals for a variety of applications such as the study of gravitational waves (Becker et al., 2018) or timing for power grid synchronization (Fuhr, 2021). Many of these proposed uses involve the navigation of spacecraft in deep space using pulsar time-of-arrival (TOA) measurements (Deng et al., 2013), which can be performed in either the radio-frequency band or the X-ray band. The main challenge for such a navigation system is the low signal strength of the pulsar signals, which can be as much as 50 to 60 dB below the noise floor. While pulsar observations on Earth can be conducted using large antennas such as the 100-meter diameter Green Bank Telescope at the Green Bank Observatory in West Virginia, a

system designed for a spacecraft would be limited to much smaller antenna apertures due to practical size and weight constraints. When using such small apertures, due to the limited antenna gain it is necessary to perform long observations and use signal processing techniques such as epoch folding to raise the signal-to-noise ratio (SNR) to a level at which the TOA measurements can be performed (Heusdens et al., 2012). Observations performed in the X-ray band require smaller antenna apertures than those performed at RF for a given accuracy and observation time. Therefore X-ray based systems have been the focus of much of the recent research into pulsar navigation (Mitchell et al., 2014; Sheikh & Pines, 2006; Shemar et al., 2016). However, despite the smaller antenna aperture, X-ray based systems require larger, heavier, and more complex hardware than RF-based systems (Mitchell et al., 2014).

While some previous studies have concluded that RF pulsar navigation systems would require antenna apertures on the order of hundreds of square meters to achieve acceptable measurement performance (Becker et al., 2013), other studies theorize that a timing accuracy of 1-10 microseconds may be feasible using a much smaller antenna with an aperture on the order of 10 square meters (Jessner, 2015; Tavares et al., 2015), which supports the idea that RF pulsars may in fact prove useful for deep-space timing and navigation purposes. In McKnight and van Graas (2022), a literature review of RF pulsar navigation concludes that there is no general consensus for the practicality of RF pulsar timing and navigation using such small antenna apertures. The large variation in results found in the literature is due to the large number of factors that must be considered for a practical system. Parameters such as effective antenna aperture, observation time, observation frequency, receiver bandwidth, receiver noise temperature, external noise sources, radio-frequency interference, pulse period and shape, geometry of the pulsar set, signal processing techniques, knowledge of error sources, and external constraints such as limited antenna pointing accuracy can each have a large effect on the theoretical performance of such a system. The wide range of performance estimates found in the literature is primarily due to variation in assumptions for these many parameters. Therefore an experimental approach such as the in-space experiment proposed in Hecht et al. (2016) is necessary in order to determine a set of reasonable specifications for a low-complexity, small-aperture system and demonstrate the validity of theoretical models.

In recent years, some experiments have been conducted on Earth using small-aperture antennas. Aided by the increasing availability of low-cost, high-performance RF hardware, many amateur radio operators around the world have demonstrated the successful observation of pulsars in the RF band using antennas with effective apertures of 5 square meters or less (Dell'Immagine, 2021; Fasching, 2021; Herrmann, 2020; Olney, 2020). These observations are typically conducted by collecting data using software defined radios and processing the data using freely available open-source software. Encouraging results have been obtained in both L-band and the UHF band using various antenna types including Yagi antennas and parabolic dishes. Given the available theoretical and experimental results, an additional study would be beneficial and could consider theoretical results and assumptions in the context of experimental results to determine feasibility limits and requirements for small-aperture RF pulsar measurements. While an in-space experiment would provide an ideal environment for the study of RF pulsar timing and navigation, as mentioned above and suggested in Hecht et al. (2016), these amateur results suggest that the design of such an experiment could be guided by preliminary terrestrial studies. These terrestrial studies would offer advantages in terms of simplicity, flexibility, and extensibility, allowing for much of the testing and performance characterization to take place on the ground before committing to an in-space experiment.

In McKnight and van Graas (2022), the preliminary design of a terrestrial small-aperture RF pulsar experiment is detailed. However, a more detailed analysis of the experiment is required before observations can be conducted. This paper describes the detailed design procedure and performance characterization of the experimental setup. The initial goal of the experiment will be to independently replicate the results obtained by the amateur radio community by demonstrating successful pulsar observations using antennas with effective apertures of less than 2 square meters. This will allow for the experimental setup to serve as a foundation for the further terrestrial study of RF pulsar signals and the validation of theoretical models of signal-to-noise ratio as a function of antenna aperture, pulsar parameters, measurement performance, and observation time. The results of the experiment will be used to guide the design of further terrestrial experiments as well as future in-space experiments. The detailed design consists of hardware selection, data collection methodology, and software architecture for initial data processing using a software-defined radio (SDR). The eventual goal is to independently demonstrate successful observations using both custom-built software and freely available open-source tools. The performance characterization of the system primarily involves the determination of the total receiver noise temperature, which along with the antenna aperture is one of the primary receiver-dependent drivers of system performance. Additionally, error sources such as dispersion and radio-frequency interference and their effect on the pulsar observations are discussed. A full consideration of these system parameters and characteristics is an important step towards the validation of theoretical performance models using the data collected by the experiment.

II. BACKGROUND

1. Key System Parameters

The key parameters governing a pulsar observation are given by the following equation (Lorimer & Kramer, 2005, p. 265):

$$\text{SNR} = \frac{SG\sqrt{n_p\Delta f t_{\text{int}}}}{T_{\text{sys}}}\sqrt{\frac{P-W}{W}} \quad (1)$$

Where:

SNR is the observed signal-to-noise ratio (unitless)

S is the pulsar mean flux density (Jy)

G is the antenna gain (K/Jy)

n_p is the number (1 or 2) of orthogonal polarizations averaged (unitless)

Δf is the pre-detection bandwidth of the receiver (Hz)

t_{int} is the total observation time (s)

T_{sys} is the total system noise temperature (K)

P is the pulse period (s)

W is the width of a single pulse (s)

The *jansky* (Jy) is a unit of spectral flux density that is commonly used in radio astronomy, where $1 \text{ Jy} = 10^{-26} \text{ W m}^{-2} \text{ Hz}^{-1}$. The representation of antenna gain in units of K/Jy is also common to radio astronomy, and is defined as follows: (p. 263)

$$G = A_e/2k_B \quad (2)$$

Where:

G is the antenna gain (K/Jy)

A_e is the effective aperture of the antenna (m^2)

k_B is the Boltzmann constant: $1.381 \times 10^{-23} \text{ J/K}$ or $1381 \text{ Jy m}^2/\text{K}$

T_{sys} can be expressed as a sum of the individual contributions from multiple independent sources of system noise (p. 263):

$$T_{\text{sys}} = T_{\text{rec}} + T_{\text{spill}} + T_{\text{atm}} + T_{\text{sky}} \quad (3)$$

Where:

T_{sys} is the total system noise temperature (K)

T_{rec} is the receiver noise temperature (K)

T_{spill} is the spillover noise temperature (K)

T_{atm} is the atmospheric noise temperature (K)

T_{sky} is the sky background noise temperature (K)

T_{rec} can in turn be calculated by modeling the receiver as a collection of linear two-port components connected in series using the Friis equation:

$$T_{\text{rec}} = T_1 + \frac{T_2}{G_1} + \frac{T_3}{G_1 G_2} + \dots \quad (4)$$

Where T_1, T_2, \dots are the noise temperatures and G_1, G_2, \dots are the gains of each successive component of the receiver, respectively. This equation can be rewritten in the following form to emphasize the specific contribution of each individual component of the receiver to the overall value of T_{rec} :

$$T_{\text{rec}} = T_{\text{rec},1} + T_{\text{rec},2} + T_{\text{rec},3} + \dots \quad (5)$$

Where:

$$\begin{aligned}
T_{\text{rec},1} &= T_1 \\
T_{\text{rec},2} &= T_2 / G_1 \\
T_{\text{rec},3} &= T_3 / G_1 G_2 \\
&\text{etc.}
\end{aligned}$$

2. Error Sources

The ionized interstellar medium (ISM) introduces a frequency-dependent delay to electromagnetic radiation that propagates through it (Lorimer & Kramer, 2005, p. 85). The time delay between two frequencies f_1 and f_2 (in MHz) is given by

$$\Delta t \approx 4.15 \times 10^6 \times (f_1^{-2} - f_2^{-2}) \times \text{DM} \quad (6)$$

where the dispersion measure (DM) quantifies the electron density along the line of sight to the pulsar and is expressed in units of cm^{-3}pc where pc denotes parsecs, a unit of distance common to astronomy. The simplest method for mitigating this effect is referred to as incoherent de-dispersion, which involves splitting the signal bandwidth into a number of frequency channels, each of which are corrected with a time delay and recombined into a de-dispersed time series (p. 109).

Lower frequencies are more affected by dispersive delay. The pulsar B0329+54, as an example, has a DM of $26.76 \text{ cm}^{-3}\text{pc}$ and an approximate pulse width of 6.6 ms (Australia Telescope National Facility, 2021; Manchester et al., 2005). Using the equation above, a center frequency of 1420 MHz, and assuming a bandwidth of 10 MHz, Δt is 0.78 ms from one end of the bandwidth to the other. This is considerably less than the pulse width, and therefore does not significantly smear the pulse in frequency. At a center frequency of 436 MHz, using the same bandwidth, Δt is found to be 26.81 ms, which far exceeds the pulse width and requires de-dispersion to maintain the shape of the pulse.

Another method for de-dispersion that should be mentioned is coherent de-dispersion, which essentially involves modeling the transfer function of the dispersive effect of the ISM

$$H(f_0 + f) = e^{i \frac{2\pi D}{(f+f_0)f_0^2} \text{DM} f^2} \quad (7)$$

and multiplying the incoming signal by the inverse of this transfer function to produce a de-dispersed time series.

$$V_{\text{int}}(f) = V(f)H^{-1}(f_0 + f) \quad (8)$$

where D in Equation 7 is a fixed constant and f_0 is the center frequency of the observation (Lorimer & Kramer, 2005, p. 119). One advantage to coherent de-dispersion is the improved time resolution of the corrected signal, since there is no discrete frequency binning in this method.

Another important error source to consider is the spillover temperature (T_{spill} in Equation 3) for a particular antenna. T_{spill} , for a dish antenna, is the total noise temperature associated with the portion of the antenna beam that “spills” over the edge of the dish and sees a noise source such as the warm Earth (assumed 290 K). For a Yagi antenna, the total noise temperature associated with the side- and back-lobes of the antenna is analogous to T_{spill} . Lorimer and Kramer (2005, p. 263) states that an approximation of 10 K or less for T_{spill} is typically appropriate, but care must be taken to ensure that this holds true for a given antenna. This assumption may not hold for small dishes with low aperture efficiency, or Yagi antennas, which often have significant back- and side-lobes in their patterns. Figure 1 depicts an example of an antenna pattern for a UHF Yagi antenna, illustrating that the portion of the radiation pattern outside the main beam is not insignificant and may warrant closer inspection.

III. DETAILED EXPERIMENT DESIGN

1. Radio-Frequency Interference Site Survey

Site surveys were conducted at both candidate antenna installations (shown in Figures 2 and 3) to determine if nearby interference could significantly reduce system performance at either location. As mentioned in McKnight and van Graas (2022), the two stations under consideration for this experiment are a 1.9 m mesh dish located at the Ohio University airport in Albany, OH, and a dual-Yagi installation on the roof of Stocker Center in Athens, OH. Low-noise amplifiers (LNAs) were installed at the feeds of both stations and data was recorded while performing a full azimuth and elevation sweep.

The Yagi installation was found to be significantly affected by strong harmonics from local FM radio transmitters. These transmissions are constant and considerably raise the noise floor at this station, severely impacting its ability to recover weak pulsar signals. The spectrum at the dish installation, while cleaner than that of the Yagi station, was also affected by multiple

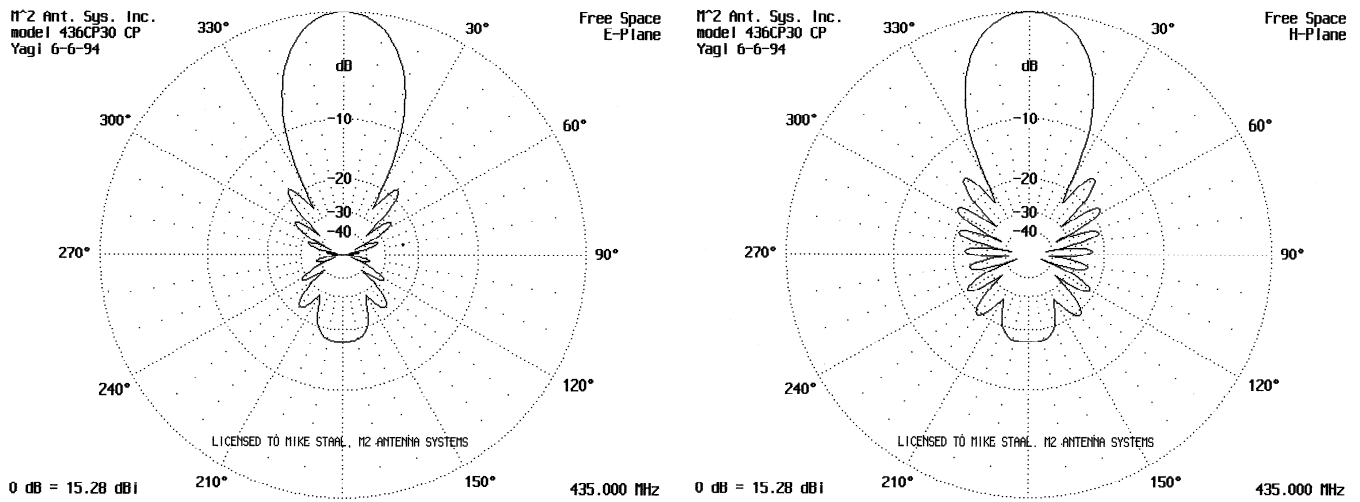


Figure 1: Radiation pattern plots for 436CP30 Yagi antenna. Plots provided by M2 Antenna Systems, Inc. and used with permission.



Figure 2: 1.9 m diameter parabolic dish located at the Ohio University Airport in Albany, OH



Figure 3: Bobcat-1 ground station located on top of Stocker Center in Athens, OH

significant sources of intermittent interference. Ultimately it was determined that the interference observed at both stations in their current configurations sufficed to raise the noise floor to a level at which successful observations would not be possible. In light of this, the decision was made to relocate the dish station to a nearby site located in a more remote area, which should result in a significantly cleaner RF environment. Therefore the analysis presented in the remainder of this paper assumes the system parameters of the dish station.

2. Hardware Selection

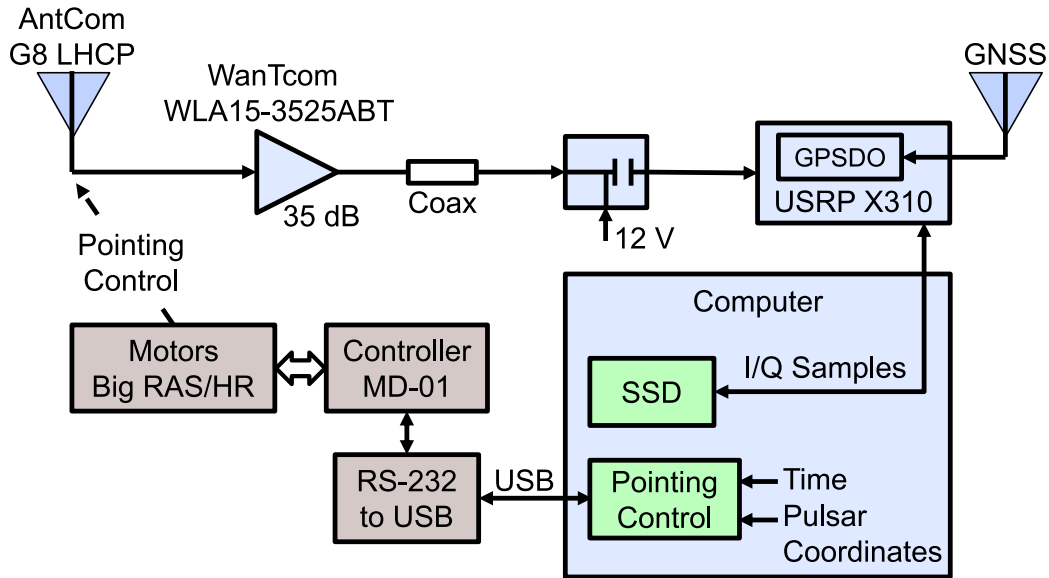


Figure 4: Block diagram of the RF hardware system

The strength of pulsar signals is typically greater at lower frequencies. A center frequency of 1420 MHz was selected for the experiment. This frequency is commonly used for radio astronomy. It typically features minimal RFI, and many amateurs have previously observed pulsars on this frequency. Additionally, it falls within the lower-end of the dish feed bandwidth. For future experiments, it may be beneficial to replace the dish feed with one covering lower frequencies to take advantage of the greater signal strength seen at these frequencies.

Figure 4 depicts the design of the hardware configuration for the system. Along with the antenna, the low-noise pre-amplifier is one of the most important components in terms of its effect on the system performance. It is imperative to select an amplifier with high gain and low noise figure. Additionally, it is important to have high stability, due to the potential for reflected power from downstream filters, and high linearity to prevent unwanted mixing of interference into the band of interest. The WanTcom WLA15-3525A low-noise amplifier was selected as the pre-amplifier for this experiment. It features a noise figure of approximately 0.4 dB at 1420 MHz, along with a gain of 35 dB and excellent wide-band linearity and stability.

Another important component of system performance is the effective bandwidth of the system. The sampling rate of the SDR provides an upper limit to this bandwidth via the Nyquist sampling theorem. However, in practice the bandwidth is additionally limited by band-pass filtering downstream from the pre-amplifier, which is necessary to prevent aliasing of signals from outside the band of interest. These out-of-band signals can manifest as additional system noise or RFI, significantly reducing the total signal-to-noise ratio of the observation. An ideal filter for this purpose would feature a sharp roll-off in order to maximize the usable bandwidth of the system while also providing strong rejection of signals in the stop-band. Many amateur setups use cavity filters or custom home-built interdigital filters, which are well-suited to these requirements.

A USRP X310 with a TwinRX daughterboard was selected as the SDR for the experiment. It supports a sample rate of 100 Msps and an RF bandwidth of 80 MHz. The TwinRX daughterboard features a sophisticated RF frontend, including integrated bandpass filtering, removing the need to add an additional bandpass filter to the system. Additionally, it supports center frequencies ranging from 10 to 6000 MHz. The high system bandwidth enabled by this choice of SDR will significantly improve the overall signal-to-noise ratio of the observations, as shown by Equation 1.

3. Software Architecture

The data collection architecture developed for this experiment follows a common methodology employed by many amateur radio astronomers, in which the baseband pulsar signal is sampled using a software-defined radio and pre-processed by separating it into a number of frequency channels to enable later incoherent de-dispersion (see Section II.2), integrating it to reduce the sampling rate, and then storing it to a file for later post-processing. The data is stored in the SIGPROC Filterbank file format, a standard format used by many freely-available pulsar software utilities. This provides the flexibility to leverage existing pulsar post-processing tools such as PRESTO or a custom post-processing implementation using MATLAB or other custom-built software.

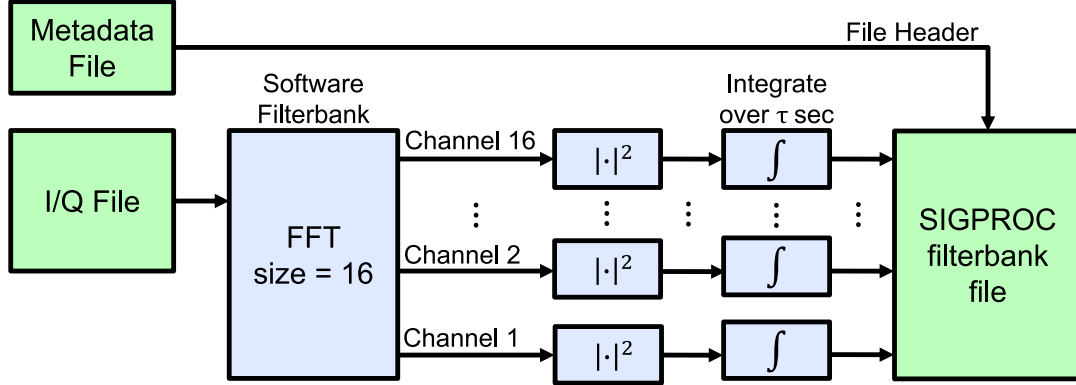


Figure 5: Block diagram of the data preprocessing software

The software pre-processing architecture is depicted in Figure 5. The first stage involves computing the magnitude of the Fourier transform over n_{chan} samples to create n_{chan} separate frequency channels. The pre-processing software in this experiment is configured to use 16 frequency channels, selected to provide adequate frequency resolution when de-dispersing the channels in post-processing. Higher numbers of channels also provide greater resolution for RFI mitigation in post-processing, as a particular channel can easily be blanked out for a period of time if interference is detected. The frequency-binned samples are then integrated over a time period of τ seconds by computing the average of each successive group of $\tau f_s/n_{\text{chan}}$ consecutive samples, channel-by-channel, which reduces the amount of data that must be stored at the cost of some time resolution. This method of forming discrete frequency bins introduces spectral leakage between frequency channels that can reduce the overall SNR. A potential point of improvement lies in implementing a convolving filter bank similar to the one described in van Straten and Bailes (2011).

4. System Performance Characterization

The total integration time required to observe a given pulsar with a reasonable signal-to-noise ratio can be calculated using the equations given in Section II.1. With the receiver hardware components selected, the receiver noise temperature T_{rec} can be calculated using Equation 5 and the parameters enumerated in Table 1 as 38.3 K.

Table 1: Parameters for Receiver Noise Figure Calculation

	Line Loss Before LNA	WanTcom WLA15-3525ABT	Cable Loss	USRP X310 TwinRX
G_i (dB)	-0.1	35.0	-10.0	35.0
NF_i (dB)	0.1	0.4	10.0	5.0
$T_{\text{rec},i}$ (K)	6.8	28.6	0.8	2.0

The process given in McKnight and van Graas (2022) can be used to calculate the integration time needed to observe various pulsars from this station given the receiver parameters and a system bandwidth of 80 MHz. The three easiest pulsars to observe in terms of integration time are given in Table 2.

According to these calculations as shown in the table, pulsar B0329+54 should be easily observable in less than 2 hours of integration time using this system.

Table 2: Best pulsar candidates for observation from the parabolic dish station at 1420 MHz

Pulsar Name (B1950)	S_{1420} (mJy)	P_0 (s)	W_{50} (ms)	T_{sky} (K)	T_{sys} (K)	Daily Visibility at 39°N Latitude (hr)	Observation Time for SNR = 10 dB (hr)
B0329+54	198.4	0.715	6.6	4.3	52.5	12.33	1.31
B0950+08	98.2	0.253	8.9	3.2	51.5	7.58	20.18
B1933+16	56.9	0.359	6.0	5.7	54.0	8.58	30.84

IV. CONCLUSIONS AND FUTURE WORK

The analysis shown in this paper has concluded that the experimental setup as designed should be sufficient to perform observations of B0329+54, the strongest observable pulsar in the Northern Hemisphere. Work is currently underway to construct the system in order to experimentally verify the results of the analysis, although as mentioned in Section III.1, it will be necessary to relocate the setup to a new site with a cleaner RF environment. Data collection will commence once a suitable location has been verified to be free of significant RFI. The software architecture outlined in this paper closely follows the design of existing amateur systems in an attempt to replicate their previous success. Once a working system has been established, it can be used as a foundation to systematically test improvements to the architecture. During the course of the analysis, several potential points of improvement were identified. Installing a lower-frequency feed on the dish or using a more sophisticated de-dispersion software algorithm, for example, could significantly improve the performance of the system. The expectation is that these improvements, among others, will be implemented for future iterations of the experiment.

V. ACKNOWLEDGEMENTS

The authors would like to thank Adam Schultz and Dr. Chris Bartone for lending hardware components to these experiments.

REFERENCES

- Australia Telescope National Facility. (2021). *The ATNF pulsar catalogue*. Retrieved November 22, 2021, from <https://www.atnf.csiro.au/research/pulsar/psrcat/>
- Becker, W., Bernhardt, M. G., & Jessner, A. (2013). Autonomous spacecraft navigation with pulsars. *Acta Futura* 7, 11–28. <https://doi.org/10.2420/AF07.2013.11>
- Becker, W., Kramer, M., & Sesana, A. (2018). Pulsar timing and its application for navigation and gravitational wave detection. *Space Science Reviews*, 214(1), 30. <https://doi.org/10.1007/s11214-017-0459-0>
- Condon, J. J., & Ransom, S. M. (2016). *Essential radio astronomy*. Princeton University Press.
- Dell’Immagine, A. (2021). *IW5BHY*. Retrieved January 9, 2021, from <http://iw5bhy.altervista.org>
- Deng, X. P., Hobbs, G., You, X. P., Li, M. T., Keith, M. J., Shannon, R. M., Coles, W., Manchester, R. N., Zheng, J. H., Yu, X. Z., Gao, D., Wu, X., & Chen, D. (2013). Interplanetary spacecraft navigation using pulsars. *Advances in Space Research*, 52(9), 1602–1621. <https://doi.org/10.1016/j.asr.2013.07.025>
- Fasching, H. (2021). *PULSARS*. Retrieved January 9, 2021, from <https://www.qsl.net/oe5jfl/pulsar/pulsar.htm>
- Fuhr, P. (2021). Pulsars as next generation grid timing sources. *Proceedings of the 52nd Annual Precise Time and Time Interval Systems and Applications Meeting*, 356–375. <https://doi.org/10.33012/2021.17774>
- Hecht, M., Cahoy, K., Fish, V., Yoon, H., Svitek, T., & Lind, F. (2016). *A tall ship and a star to steer her by*. MIT Haystack Observatory.
- Herrmann, W. (2020). Pulsar observation with a 3-m dish. *Journal of the Society of Amateur Radio Astronomers*, 60–69.
- Heusdens, R., Engelen, S., Buist, P. J., Noroozi, A., Sundaramoorthy, P., Verhoeven, C., Bentum, M., & Gill, E. (2012). Match filtering approach for signal acquisition in radio-pulsar navigation. *63rd International Astronautical Congress*, 1–5.
- Jessner, A. (2015). Technical requirements for autonomous space craft navigation using radio pulsars. *Proceedings of the 593rd WE-Heraeus Seminar on Autonomous Spacecraft Navigation*.
- Lorimer, D., & Kramer, M. (2005). *Handbook of pulsar astronomy*. Cambridge University Press.

- Manchester, R. N., Hobbs, G. B., Teoh, A., & Hobbs, M. (2005). The Australia Telescope National Facility pulsar catalogue. *Astronomical Journal*, 129(4), 1993–2006. <https://doi.org/10.1086/428488>
- McKnight, R., & van Graas, F. (2022). Radio-frequency pulsar observation using small-aperture antennas. *Proceedings of the 2022 International Technical Meeting of The Institute of Navigation*, 856–866. <https://doi.org/10.33012/2022.18259>
- Mitchell, J. W., Hassouneh, M. A., Winternitz, L. M., Valdez, J. E., Ray, P. S., Arzoumanian, Z., & Gendreau, K. C. (2014). Station explorer for X-ray timing and navigation technology architecture overview. *Proceedings of the 27th International Technical Meeting of the Satellite Division of The Institute of Navigation (ION GNSS+ 2014)*, 3194–3200.
- Olney, S. (2020). *Neutron Star Group*. Retrieved November 11, 2020, from <http://neutronstar.joataman.net>
- Rawley, L., Stinebring, D., Taylor, J., Davis, M., & Allan, D. W. (1986). Millisecond pulsar rivals best atomic clock stability. *Proceedings of the 18th Annual Precise Time and Time Interval Systems and Applications Meeting*, 453–466.
- Sheikh, S. I., & Pines, D. J. (2006). Recursive estimation of spacecraft position and velocity using X-ray pulsar time of arrival measurements. *NAVIGATION: Journal of The Institute of Navigation*, 53(3), 149–166. <https://doi.org/10.1002/j.2161-4296.2006.tb00380.x>
- Shemar, S., Fraser, G., Heil, L., Hindley, D., Martindale, A., Molyneux, P., Pye, J., Warwick, R., & Lamb, A. (2016). Towards practical autonomous deep-space navigation using X-Ray pulsar timing. *Experimental Astronomy*, 42(2), 101–138. <https://doi.org/10.1007/s10686-016-9496-z>
- Tavares, G., Brito, D., & Fernandes, J. (2015). A study on the accuracy of radio pulsar navigation systems. *Proceedings of the European Navigation Conference 2015 (ENC 2015)*.
- van Straten, W., & Bailes, M. (2011). DSPSR: Digital signal processing software for pulsar astronomy. *Publications of the Astronomical Society of Australia*, 28(1), 1–14. <https://doi.org/10.1071/AS10021>